Astron. Astrophys. 236, 362–370 (1990)

ASTRONOMY AND ASTROPHYSICS

High-metallicity effects in *BVRI* colour-magnitude diagrams: the globular cluster NGC 6553 *

S. Ortolani [1], **B. Barbuy** [2], **and E. Bica** [3]

[1] Osservatorio Astronomico di Padova, Vicolo dell'Osservatorio 5, I-35123 Padova, Italy
[2] Universidade de São Paulo, Departamento de Astronomia, C.P. 30627, São Paulo 01051, Brazil
[3] Universidade Federal do Rio Grande do Sul, Departamento de Astronomia, C.P. 15051, Porto Alegre 91500, Brazil

Received August 18, 1989; accepted February 15, 1990

Abstract. We present *BVRI* CCD-photometry of about 15000 stars in the possibly super-metal-rich globular cluster NGC 6553. The photometry extends to $V=21.5$ reaching the cluster turn-off region. In the V vs. $(V-I)$ diagram the red giant branch forms an arc, where the red tip is as faint as the horizontal branch, due to blanketing effects which are particularly strong in the high-metallicity late-type stars Depending on the amount of blanketing in the spectral region and the combination of filters, the tip of the giant branch turns back towards the blue in certain colours like $(B-V)$. Such distributions in the colour-magnitude diagrams (CMD) might be misleadingly interpreted in terms of a scatter in metallicity.

The horizontal branch (HB) is so extremely red that it partially overlaps the red giant branch (RGB).

The shape of the RGB and the relative positions of the RGB and the HB differ significantly from those of globular clusters usually called metal-rich as, for example, 47 Tuc.

Using as age criterion the magnitude difference between the turn-off and the HB, we have estimated that the age of NGC 6553 should be slightly below that of classical globular clusters.

Key words: globular clusters – high metallicity – colour-magnitude diagrams

1. Introduction

The study of super-metal-rich populations in terms of available colour-magnitude diagrams (CMD) concern the metal-rich stars in the Baade window (Whitford and Rich, 1983; Frogel and Whitford, 1987; Terndrup, 1988) and the bulge of M31 (Mould, 1986). The difficulties of such studies come from the different ages, metallicities, reddening of the bulge stars, and in the case of our Galaxy, the additional problem of the distance. An ideal object for the study of the CMD properties of a super-metal-rich population would be a super-metal-rich cluster.

NGC 6553 = GCL 88 ($\alpha_{1950}=18^{\rm h}05^{\rm m}11^{\rm s}$, $\delta_{1950}=-25°55\farcm1$) is a low galactic latitude globular cluster ($l=5\fdg253$, $b=-3\fdg029$) toward the Galaxy center. In the classification of Zinn (1985) it belongs to the disk population of metal-rich globular clusters. Early spectral and photometric studies suggested that NGC 6553 was among the most metal-rich globular clusters in the Galaxy (Morgan, 1959; Van den Bergh, 1967). More recent photometric observations with intermediate band photometry of metallic features confirmed this picture, indicating solar or higher metallicity (Zinn, 1980a; Bica and Pastoriza, 1983; Zinn and West, 1984), although the precise [M/H] (using the standard definition $[X]=\log X_{\rm star}-\log X_{\rm sun}$) is still dependent on the photometric calibrations.

NGC 6553, as well as NGC 6440 and NGC 6528, present integrated spectra which are clearly more strong-lines than the well-studied clusters usually called metal-rich in the literature, such as 47 Tuc or NGC 6356 (Bica and Alloin, 1986a, b). The line strengths are comparable to those in the nuclei of most galaxies brighter than $M_B=-20$, although they are weaker than those found in the nuclei of most massive elliptical galaxies (Bica, 1988).

Hartwick (1975) presented a photographic BV diagram limited to $V\approx 18$, and Lloyd Evans and Menzies (1973) obtained *VI* photographic diagrams.

In this work, *BVRI* CCD photometry reaching 21.5 V magnitude stars of the globular cluster NGC 6553 is presented. Given the evidences for high metallicity of this cluster, these CMDs are important as a reference for the interpretation of super-metallic populations in such diagrams.

In Sect. 2 the observations and reductions are described. In Sect. 3 the CMDs in several magnitudes and colours are shown, and their morphologies are described. In Sect. 4 the reddening and the age are derived. In Sect. 5 the implications of our results for the super-metallic populations are discussed, and concluding remarks are given.

2. Observations

2.1. Description of data and instrumentation

The observations have been carried out with the 1.5 m Danish telescope at the European Southern Observatory (ESO) at La Silla, Chile, equipped with the high resolution RCA CCD no. 8, of $15\,\mu^2$ pixel size. The field is about $4' \times 2\farcm5$. The set up of the CCD was carefully adjusted in order to minimize the low level non-

Send offprint requests to: S. Ortolani

* Based on observations collected at the European Southern Observatory (ESO), La Silla, Chile.

Table 1. Log-book of the observations obtained at the 1.5 m Danish Telescope at ESO, La Silla, Chile

Filter	Date	U.T.	Exposure time (s)	Seeing (″)	ESO CCD no.
V	19.03.1988	08^h59^m	30	0.8	8
B	19.03.1988	09 04	1800	0.8	8
V	19.03.1988	09 40	480	0.7	8
R	19.03.1988	09 50	300	0.7	8
B	21.03.1988	09 28	600	1.0	3
V	21.03.1988	09 40	300	1.0	3
R	21.03.1988	09 47	180	0.95	3
V	21.03.1988	09 15	300	1.0	8
B	24.03.1988	09 22	600	1.1	8
I	24.03.1988	09 40	60	1.3	8
V	26.03.1988	08 23	120	0.8	8
B	26.03.1988	08 27	360	0.9	8
R	26.03.1988	08 36	60	0.8	8
Field at 6′ north of NGC 6553:					
B	30.05.1986	08^h07^m	1800	1.9	1
V	30.05.1986	08 40	600	1.9	1
R	30.05.1986	09 01	300	1.9	1

linear columns and the readout noise, two fundamental conditions for our high resolution, short exposure frames. The final result was a very smooth field with a residual spatial noise of 0.5 to 0.6% and a readout noise of about 30 electrons. The gain of $5\,e^-$/ADU was chosen for frames where faint stars had to be measured, while $10\,e^-$/ADU was selected when the widest dynamic range was the main requirement.

A residual, non-uniform slope in the *Y* (north-south) direction of the background, due to a sensitivity variation across the chip was present: 1.5% in *B*, 2% in *V*, 22% in *R* and 47% in *I*. We obtained some good images with the RCA CCD ESO no. 3, of $30\,\mu^2$ size. Table 1 summarizes the observations used and Fig. 1 shows a *V* image of the cluster, where the variable stars are identified.

Background field frames in *B*, *V* and *R* were obtained in 1986, at 6′ north of the cluster, using the former low resolution RCA CCD ESO no. 1, covering the same projected field size.

The detailed *BVRI* photometric data for the list of 15.000 stars will be presented in a separate publication.

2.2. Reductions – selection

The strong background intensity slope, in the red, of the CCD no. 8 required a careful reduction. After a check with standard star observations, we concluded that this effect was due to a sensitivity gradient and not to scattered light. Normal dome flatfields taken according to the ESO CCD Danish manual, do not reproduce very well such feature, still leaving a residual of about 1% after normal flatfield division. Twilight sky background flatfields were then used for a better flatfielding, by previously fitting a polynomial surface in order to minimize any noise increase. Then high frequency components were corrected via dome flatfield division.

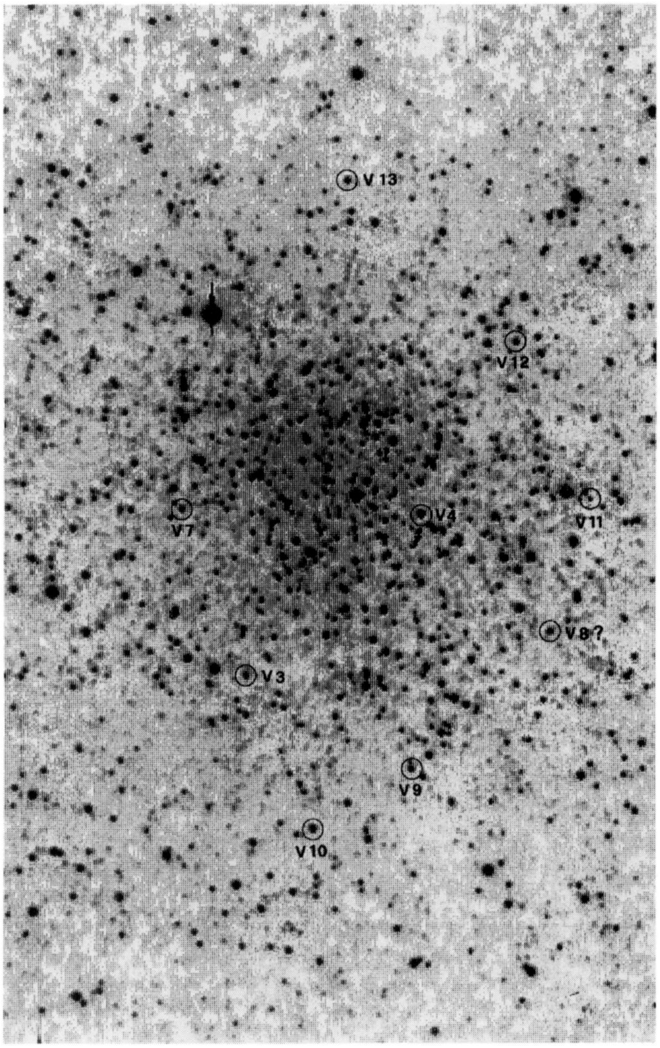

Fig. 1. *V* image of the cluster. The variable stars are identified by circles. The field is about 3′ × 4′. North is up and west to the left

Stellar photometry of the single stars was obtained at the ESO-Garching computing center using the Romafot and Daophot packages loaded on the Vax 8600 environment. Given the considerable amount of processing time involved, the relatively faster reductions using Daophot were preferred, whereas Romafot was used, with clearly better results, only for the central, very crowded regions. Only the images of 18, 23 and 26 March 1988 were used, given the good seeing of the first set, and the high dynamic range of the other two.

2.3. Calibration

The calibration of such a crowded field, containing very red stars was not an easy task. Intensive observations of standard stars from Landolt (1983) in the widest colour range, carried out during several runs from March 1988 to April 1989, using the same CCD and filters, allowed us to conclude that the calibration can be extrapolated to very red stars of $(B-V)$ up to 2.0 or 2.2, without substantial variation of the colour coefficients in the *B* and *V* bands. In the *R* and *I* bands the colour term correction is negligible. The final standard calibration, derived from 30 observations of Landolt stars are:

$B = 24.69 + 0.11\,(B-V) + b$

$V = 25.19 + 0.04\,(B-V) + v$

$R = 23.96 + r$

$I\ = 22.69 + i$

where capital letters are for Johnson-Cousins calibrated magnitudes, and low-case letters are instrumental magnitudes obtained from 20×20 pixels (or 40×40 pixels at high resolution; high resolution means that the CCD was used in the full resolution mode (15 μ pixel) and not in the binned 2×2 mode of the other observations, corresponding to a resolution with the "standard" 30 μ pixel) IHAP aperture photometry. The $(B-V)$ colour of these standards ranges from -0.17 to 1.97. The final calibration of NGC 6553 stars was obtained by transfer of the aperture magnitudes to bright, relatively uncrowded stars around the cluster. The instrumentally fitted magnitudes, as compared to the aperture ones, give a scatter of about 0.07 to 0.15 mag around the average, probably due to blend effects. The accuracy of our calibration should then be considered limited by this quantity.

A negligible error on the average is found from frame comparison: about 0.04 to 0.06 for $V = 15$ to 18 mag, and 0.05 to 0.08 in $(B-V)$. It rises to $\Delta V = 0.12$ and $\Delta(B-V) = 0.18$ at the limit $V = 19$–20 mag, in excellent agreement with the theoretical propagation of the errors from single B or V to the combined $(B-V)$. It has to be noted that this error should be reduced by a factor squareroot of 2, because it is done with the difference of two frames. These errors are about 50% higher than the theoretical errors given by Daophot, where the crowding effects are ignored, taking into account only the statistical errors.

In the reductions done for the deepest frames, where the turnoff is detected, it is not possible to use the intercomparison; in this case the Daophot errors are of 0.02 to 0.03 mag until $V = 15$ to 20.5 mag, rising to 0.08 mag in B and in V, at $V = 21$ mag on the main sequence. This means an error of 0.11 to 0.12 in the $B-V$ or probably 50% more if crowding errors are taken into account, at the limit of the photometry. In view of this analysis, we estimate that we do not have a photometric error higher than 0.06 in V and 0.1 in $(B-V)$, around the turn-off ($V \approx 20$).

The contribution of (a) contamination, (b) residual differential reddening, (c) blends not separated in two different frames (i.e., an extra-crowding effect not taken into account when comparing two slightly different frames), makes the final error at the turn-off much higher. A very approximate estimate of the total error for such faint stars would be around 0.2 to 0.3 mag.

A comparison with photometric data by Hartwick (1975) shows that the agreement in $(B-V)$ is good, with a shift of less than a few hundredths of a magnitude, but a slope is evident in V. The difference is negligible for bright stars ($V = 14, 15$), with the same zero point within ± 0.1 mag, but it seems that Hartwick's photometry is not linear below $V \approx 16$, showing deviations up to 0.5 to 1.0 with respect to our CCD photometry.

The linearity of the CCD was checked by comparing the deepest V frame (8 min) with a less exposed one (5 min) used for measuring the magnitude of the brightest stars. It appears that a difference in magnitude is practically constant, around zero, for $V \gtrsim 15.7$, whereas a tendency to systematically fainter magnitudes, of the order of $\Delta V \lesssim 0.05$ mag is present for $V \lesssim 15.7$ in the deepest frame photometry, as it approaches the saturation.

3. Colour-magnitude diagrams (CMDs)

3.1. Background and cluster fields

We show in Fig. 2a the CMD of the field background located 6′ north of NGC 6553. The cluster CMD for equal field size (2.′5 × 4′) is given in Fig. 2b.

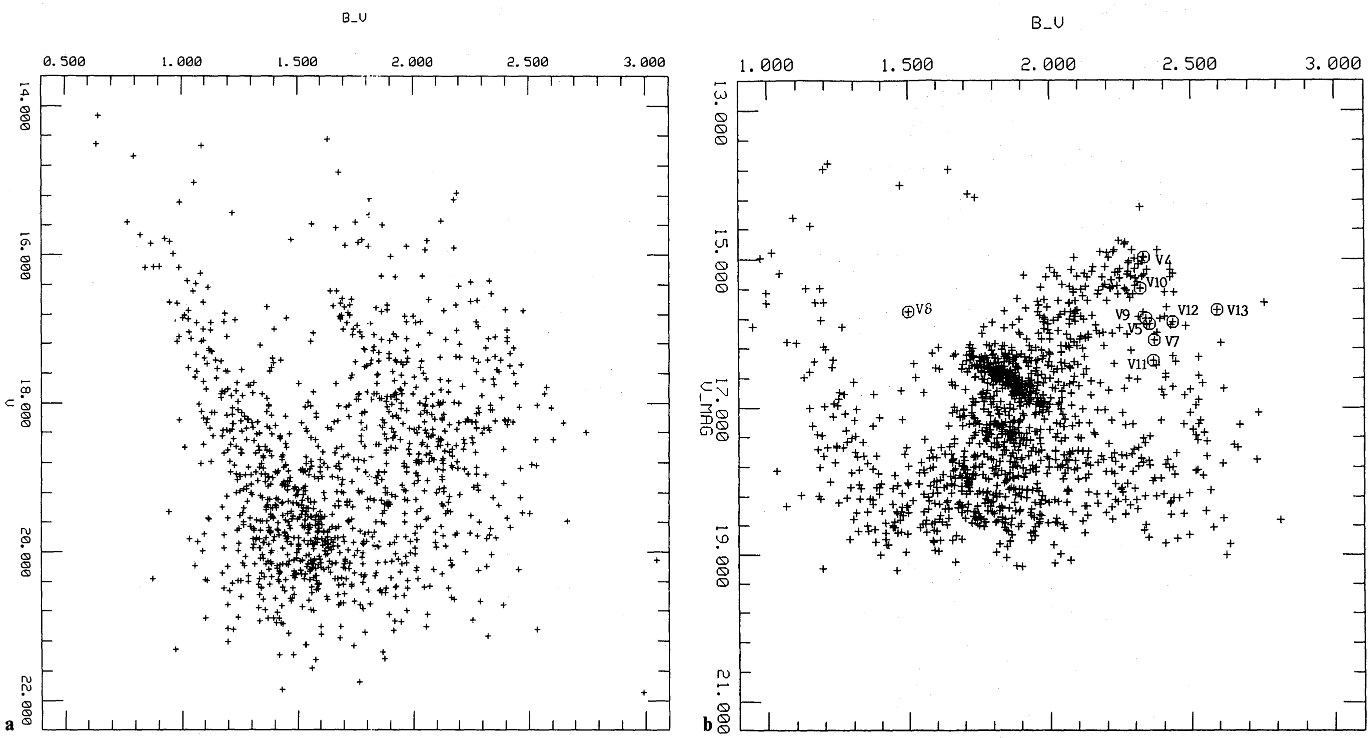

Fig. 2. **a** Field CMD at 6′ north of the cluster center; **b** cluster CMD for equal size as background (2.′5 × 4′). The variable stars are identified in **b**

The background field CMD is very similar to that of the Baade window and that of the $-6°$ galactic latitude CMDs published by Terndrup (1988). We see a blue branch which is probably a main sequence (MS) of a younger component and a red branch consisting of older evolved stars. In particular, a feature at $V \approx 16.8$ and $(B-V) \approx 1.7$ resembles a red HB. All these features are also present in the whole field for the cluster. The blue MS overlaps with the expected position of possible blue stragglers. Since it is quite evident that the blue stars of the cluster fields are much less numerous than in the background field, due to crowding losses, one should be careful in judging about the presence of blue stragglers. The position of the supposed red HB is consistent with that of the red HB of the Baade window and of the $-6°$ field (Terndrup, 1988). It has about the same colour as the cluster HB: at $(B-V)=1.7$, $V(\mathrm{HB}) \approx 16.3$ for the cluster [see Sect. 4b for a more detailed discussion of V(HB)]. Therefore, this estimated difference in magnitude of $\Delta V=0.5$ locates the cluster 4.9 kpc from us and 3.6 kpc from the galactic center.

3.2. The CMD morphology in different colours and magnitudes

3.2.1. Morphology of the red giant branch

Figure 3a–c giving V vs. $(B-I)$, $(V-I)$, and $(R-I)$ clearly show that the red giant branch forms an arc. Evidences for this effect in a less metal-rich cluster as NGC 5927, in V vs. $(V-I)$, appear in the work by Lloyd Evans and Menzies (1977) – see also Lloyd Evans (1983).

Our observations for NGC 6553 seem to be a particular case where the effect appears very strong, to the point that the tip of the RGB is as low in magnitude as the HB. This can be explained since the opacity of metal-rich red giant stars becomes stronger with metallicity due specially to molecular bands of TiO and ZrO (diatomic molecules involving two metals have their line strengths increasing faster than the metallicity).

The opacity is stronger in BVR than in I. As a matter of fact, a typical M 2–M 4 star shows strong molecular bands of TiO specially, from the blue to the R region, whereas only the FeH band at λ 920 nm is present in the I filter, being relatively weak in these stars (FeH becomes strong in M 7 or later type giants).

For these same reasons, the arc is also present in the CMD for the R magnitude, and indices containing I, as in Fig. 4 showing R vs. $(B-I)$.

On the other hand, in cases where the index contains other combinations of colurs, as BVR, given that the opacity is strong in all of them, the arc is wider and less evident. An example is shown in Fig. 5, giving V vs. $(V-R)$ – see also Fig. 2 giving V vs. $(B-V)$.

A selection of stars clearly belonging to the RGB was done. The stars were identified and extracted from the V vs. $(V-I)$ diagram (Fig. 3b). These high probability members are suitable for a detailed spectroscopic study in view of a precise determination of the cluster metallicity, it can be seen in Fig. 3b that the arc is clearly present, but it is less pronounced or disappears in the V vs. $(B-V)$ diagram (Fig. 2b). It appears that the tip of the RGB turns back to the blue, and reaches the ascending RGB. Therefore, this single-metallicity RGB becomes very wide and can be misleadingly interpreted: in the bulge of M31, for example, a wide giant branch is observed. In the literature this has been attributed entirely to a metallicity dispersion, and this might not be the case.

Figure 6 shows that, in the I vs. $(V-I)$ diagram, the RGB is always ascending: neither the arc nor the turn-back is observed. These stars are very luminous in I, also because the opacity is not strong, but it is mainly due to the stellar temperatures.

In Fig. 7 giving I vs. $(B-V)$, the RGB is always ascending; the turn-back is present but at the high I magnitudes. In this case no overlapping with other less evolved giants occurs, as in the case of Fig. 2b.

As a caution to observations of spheroids of massive galaxies, to be done with the Space Telescope, for example, we suggest that: given that the form of the RGB is more clear in CMDs including the magnitude I, the determinations of metallicity dispersions and distance might be more suitably obtained with diagrams such as I vs. $(B, V, R-I)$. On the other hand, the curvature of the arc in diagrams such as V vs. $(B, V, R-I)$ can possibly be used as a metallicity indicator, if the metallicity dispersion is small.

Concerning the presence of an asymptotic giant branch (AGB), it cannot be distinguished from the RGB in any of the CMDs. The AGB stars might be superimposed on the RGB, contrarily to 47 Tuc, for example, where the two sequences (RGB, AGB) are well separated (Hesser et al., 1987).

3.2.2. Morphology of the horizontal branch (HB)

A very interesting feature in the diagrams is the position of the HB. The HB of NGC 6553 is very red, partly overlapping the RGB, and in some of the diagrams crossing the RGB – see Fig. 7. For a comparison, in 47 Tuc, there is a gap of 0.1 mag in $(B-V)$ between the red HB and the RGB (Hesser et al., 1987; Aurière and Ortolani, 1988).

Also, as seen in Figs. 3a–c, for example, the HB of NGC 6553 is very peculiar: it is tilted, a phenomenon also present in clusters like NGC 6760 and NGC 6539 (Armandroff, 1988).

In addition to the HB, at approximately the same magnitude, there might be present a clump of ascending RGB stars, in the phase where the hydrogen burning shell crosses the chemical discontinuity left by the convective envelope.

We have inspected the magnitude of the clump locus, following King et al. (1985). It might be located up to the same level as the HB or, at the other extreme, 0.5 mag below it. Consequently, the extended HB that we see could be partly due to the clump. The tilting as well might be due to the presence of the clump.

A second possibility for the tilting comes from the blanketing effects affecting the magnitude differentially along the HB, depending on the stellar temperature. Using bolometric corrections from Bell and Gustafsson (1978) for stellar type G4 to K1, which correspond to the edges of the observed HB assuming solar metallicity, the blanketing effect goes from -0.41 to 0.174, therefore accounting for a tilting of $\Delta V=0.24$ mag.

Finally, Armandroff (1988) has interpreted the tilting of his clusters entirely in terms of differential reddening across the cluster field. In order to estimate the reddening vector, we have plotted the CMDs for different strips of the frame. The differential reddening is strong in the north-south direction. Figure 8 shows the approximate mean loci derived from the upper and lower strips (300 pixel wide). The shift is clearly present, and we could derive an approximate differential reddening of $E(B-V)=0.06$. The vector on the upper left corner of this figure represents the reddening vector for $\Delta V=0.3$ mag and $E(B-V)=0.1$. We see therefore that the reddening vector is essentially parallel to the extended HB. If the tilting of the HB is entirely attributed to differential reddening, then $A_v=0.5$, which corresponds to $E(B-V)=0.17$. As the RGB is clearly narrower than the HB, the differential reddening cannot alone account for the observed extension of the HB.

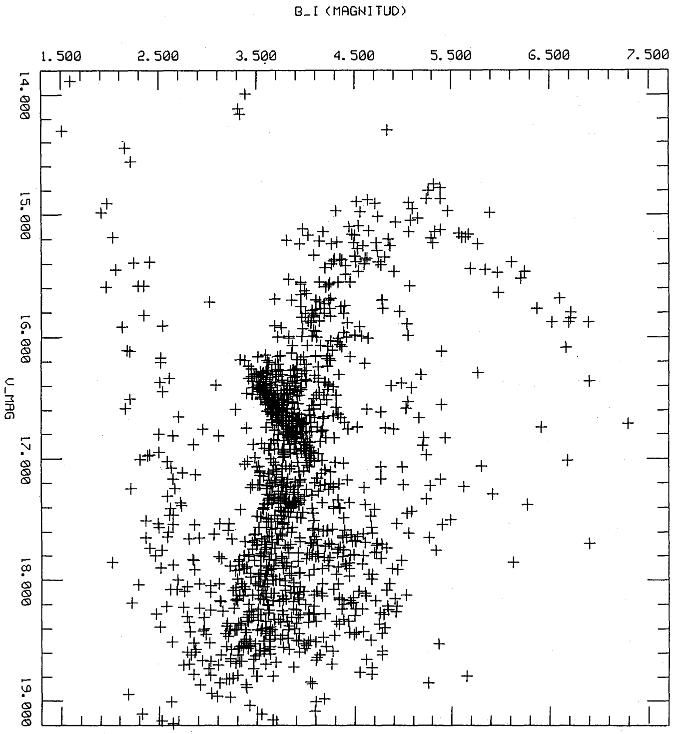

Fig. 3a

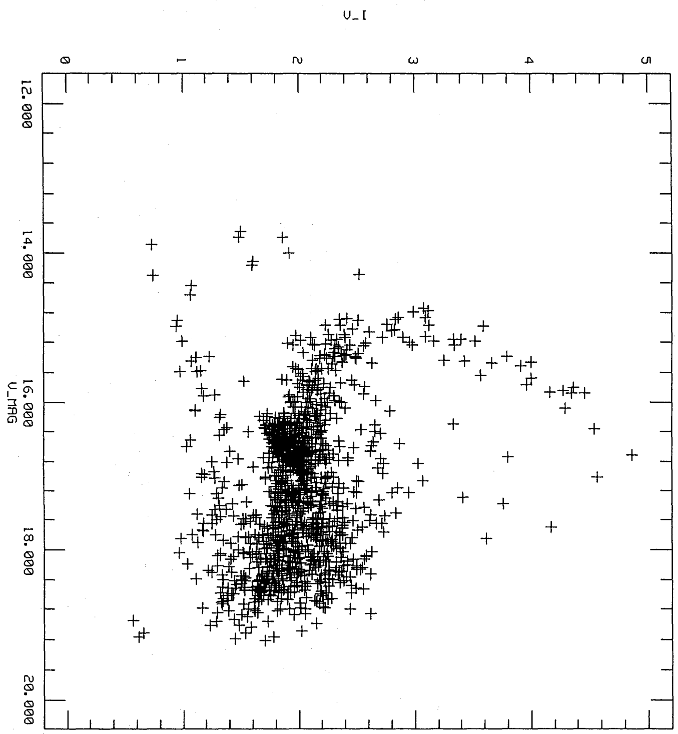

Fig. 3b

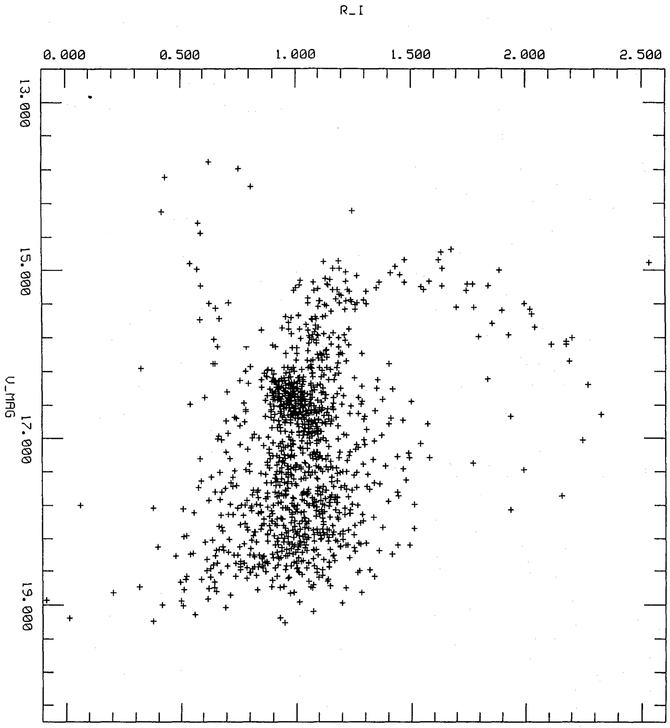

Fig. 3c

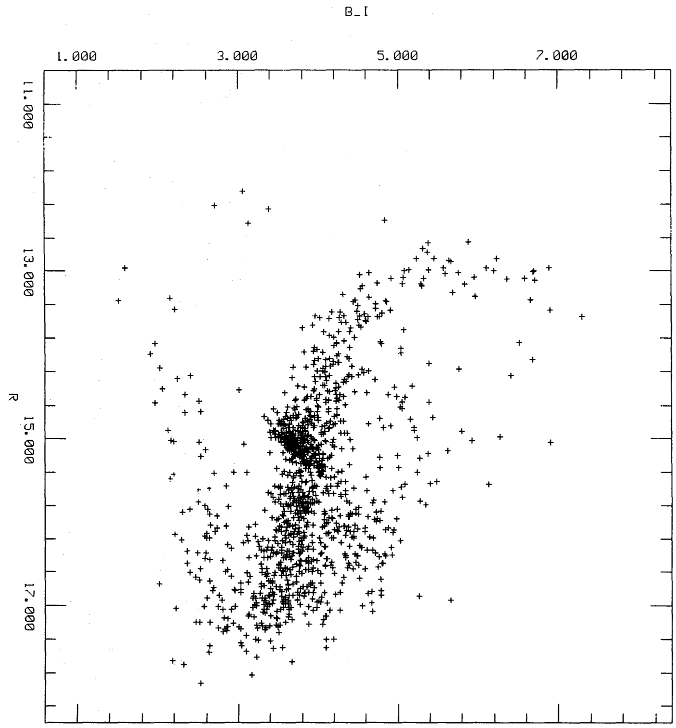

Fig. 3a–c. CMDs of brightest stars (non-saturated frames) in **a** V vs. $(B-I)$; **b** V vs. $(V-I)$; **c** V vs. $(R-I)$

Fig. 4. CMD in R vs. $(B-I)$

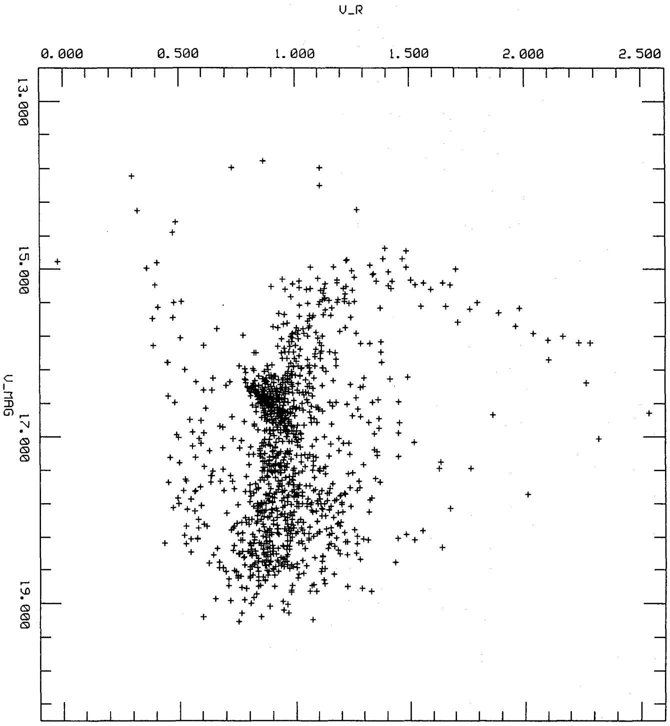

Fig. 5. CMD in V vs. $(V-R)$

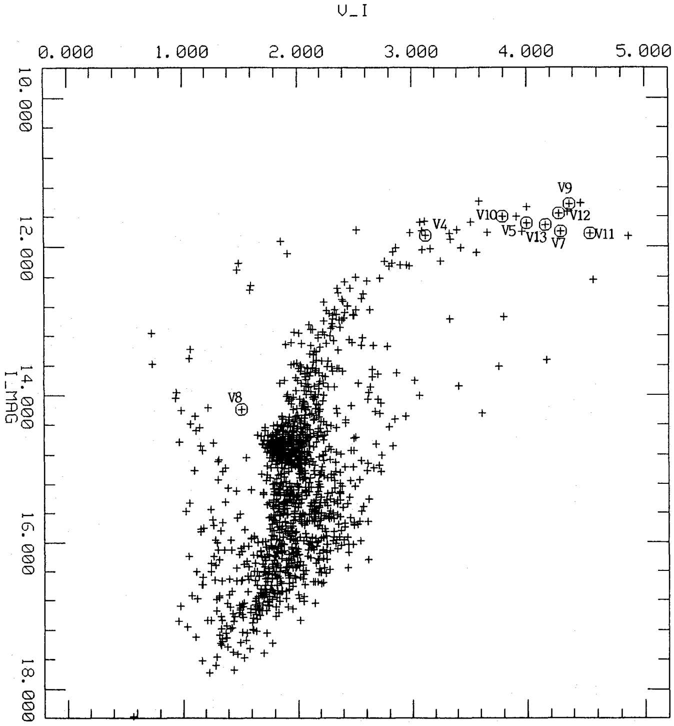

Fig. 6. CMD in I vs. $(V-I)$ for bright stars (non-saturated frame). The variable stars are identified

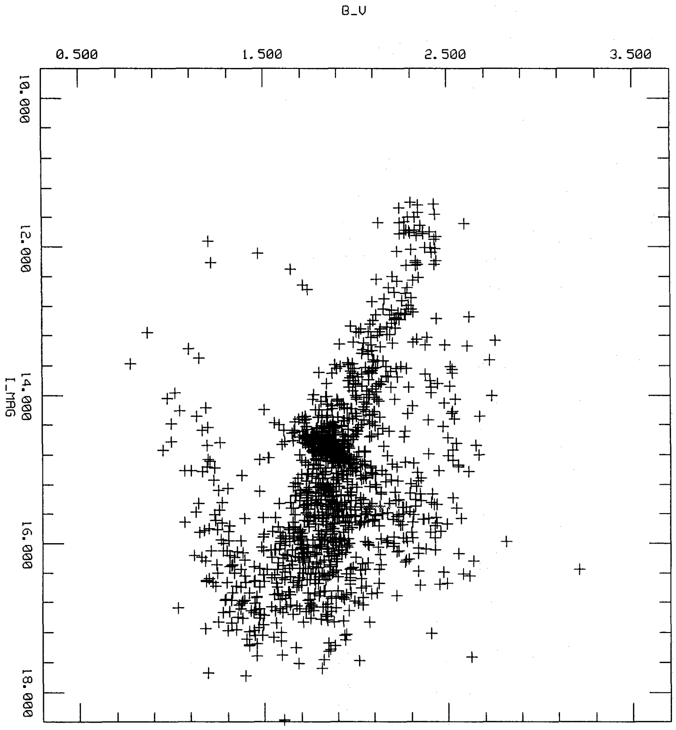

Fig. 7. CMD in I vs. $(B-V)$ for bright stars (non-saturated frame)

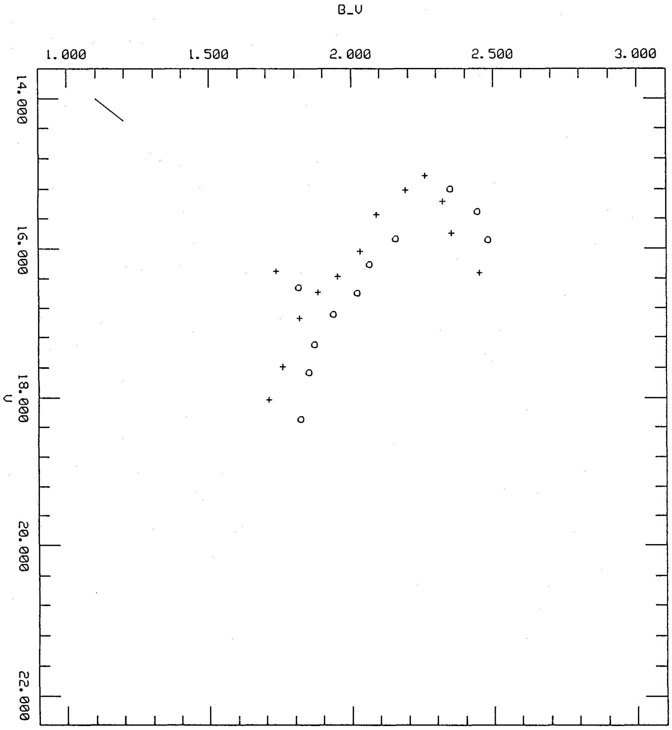

Fig. 8. Mean locus of CMD for the upper ($500 \lesssim Y \lesssim 800$ pixels) and lower ($Y \lesssim 300$) strips of frame, showing a clear differential reddening. The direction of the reddening vector is shown in the upper left corner of the figure

We conclude that differential reddening, blanketing, and also probably the presence of the RGB clump, all contribute to the peculiar form of the HB.

3.3. Variable stars

A list of variable stars identified in this cluster is summarized by Hogg (1973). For the identification of the variables on the frame, a combination of identifications in finding charts by Hartwick (1975) and by Lloyd Evans and Menzies (1973) was done. Our identifications are indicated in Fig. 1.

Figures 2b and 6 show the variable stars in the CMDs V vs. $(B-V)$ and I vs. $(B-I)$, where the non-saturated frames, used to measure the bright stars were used. It appears that V3 and V8 are non-members (if correctly identified from the ambiguous Lloyd Evans and Menzies compilation) and V4, V5, V7, V9, V11, V12, V13, V14 are probable members. V3 is only seen in the deepest frames, given its faintness, and is not indicated in Figs. 2b and 6: since this RR Lyrae is non-member, it seems that the cluster has no RR Lyrae identified.

4. Age and reddening

As we are possibly dealing with a super-metal-rich cluster, and given that appropriate isochrones are not available, we proceed to a parameter determination by a comparison with well studied metal-rich clusters. In particular, we have chosen 47 Tuc and Pal 12 because they are metal-rich, although not as much as NGC 6553, and also because we have observations obtained with the same instrumentation and reduced in the same way (Aurière and Ortolani, 1988; Ortolani, 1988; Gratton and Ortolani, 1988), showing a well defined main sequence (MS) for both clusters.

These two clusters, 47 Tuc and Pal 12 are little affected by reddening and present a significant age difference. 47 Tuc has an age typical of the old globular clusters (Buonnano et al., 1989), and Pal 12 is a globular cluster of the outer halo showing an exceptional low age (Gratton and Ortolani, 1988).

In Fig. 9a a selected V vs. $(B-V)$ diagram, suitable for age determination, is shown: it corresponds to a deep, long exposure frame, where the faintest stars can be measured, and only the lower strip of the frame ($Y \lesssim 300$ pixels) is considered, given that the reddening is relatively lower there (see Fig. 8). In this figure it can be seen that the strong concentration of points below $V=19.5$ clearly indicates the detection of the MS. The large spread could be due to field contamination, photometric imprecisions, mostly due to crowding, still some differential reddening, and metallicity spread, probably in this order. An additional problem is the background main sequence, crossing the turn-off at its upper part. Despite all these problems, the turn-off is detectable at $V=19.9\pm0.3$ and $(B-V)=1.50\pm$p.15.

In Figs. 9b and c are shown the V vs. $(B-V)$ CMD of 47 Tuc and Pal 12, to be compared to that of NGC 6553.

4.1. Reddening

We have estimated the reddening of NGC 6553 by comparing the RGB $(B-V)$ colour at the level of the HB, with that of 47 Tuc. We find $(B-V)_g=1.91\pm0.04$ for NGC 6553 and, adopting for 47 Tuc $(B-V)_g=1.03$ (Aurière and Ortolani, 1988) and $E(B-V)=0.04$ (Hesser et al., 1987), we derive $E(B-V)=0.92$.

The reddening from the turn-off colour is derived in the same way, resulting $E(B-V)=1.0$; if Pal 12 is used, then $E(B-V)=1.08$ is obtained, being slightly larger, as expected from its younger age.

The average reddening derived from the 47 Tuc comparison for the turn-off and subgiant locuses is adopted to be $E(B-V)=1.0\pm0.1$. This is an upper limit because there is a significant difference in metallicity between the two clusters (Bica and Alloin, 1986a). In other words, part of this is due to a true reddening, and part to opacity effects. If the extinction usually assigned to NGC 6553 of $E(B-V)=0.8$ is adopted (e.g., Hartwick, 1975; Zinn, 1980a; Bica and Alloin, 1986; Webbink, 1985), then 0.2 mag can be attributed to the high opacity of NGC 6553.

We stress the point of a metallicity difference between NGC 6553 and 47 Tuc, demonstrated by the following works: (i) see Zinn (1980a), Bica and Pastoriza (1983), Zinn and West (1984), Zinn (1985) for photometric work, (ii) spectroscopic work by Bica and Alloin (1986) indicate a high metallicity, although Pilachowski (1984) gives a metallicity as low as [M/H] = −0.7 dex for NGC 6553; (iii) from a preliminary inspection of a spectrum of the individual star III-17 seems to show a high metallicity.

4.2. Age

In a direct comparison of the CMDs for 47 Tuc, Pal 12 and NGC 6553, we have used the magnitude difference between turn-off and the HB ΔV(TO-HB) as age indicator.

A study of V(HB) and ΔV(TO-HB) as a function of metallicity was done by Fusi-Pecci et al. (1989), where it is shown that a difference in HB magnitude of $\Delta V(\mathrm{HB})=0.3$ mag. The important fact, as pointed out by Buonnano et al. (1988), is that the dependence of ΔV(TO-HB) with metallicity value of $\Delta V(\mathrm{TO\text{-}HB})=3.54\pm0.15$ from an homogeneous set of 17 galactic globular clusters.

In Table 2 are shown values for ΔV(TO-HB) for the clusters NGC 6553, 47 Tuc and Pal 12.

We see that NGC 6553 seems to present an age intermediate between 47 Tuc and Pal 12. However, given the error bar of ±0.25 in V(HB), an age as old as that of 47 Tuc or as young as that of Pal 12 cannot be ruled out. At face value, it seems that NGC 6553 is intermediate in age between 47 Tuc and Pal 12.

The probably slightly younger age of NGC 6553 relative to classical globular clusters might explain some of the observed peculiarities of this cluster, such as the HB morphology which resembles that of intermediate age Magellanic Cloud clusters. For a comparison, we show also in Table 2 the ΔV(TO-HB) values for ESO 121-SCO 3 and L1, clusters of the Large and Small Magellanic Clouds (LMC, SMC) respectively (Mateo et al., 1986; Olszewski et al., 1987), which show red HB and are among the oldest intermediate age clusters of these galaxies. It is surprising however that a closer similarity of HB morphology appears

Table 2. Magnitude difference between turn-off (TO) and horizontal branch (HB) used as age criterion

Cluster	ΔV(TO-HB)
47 Tuc	3.60 ± 0.1
NGC 6553	3.30 ± 0.25
Pal 12	3.10 ± 0.1
ESO 121-SCO 3	3.15 ± 0.1
L1	3.03 ± 0.1

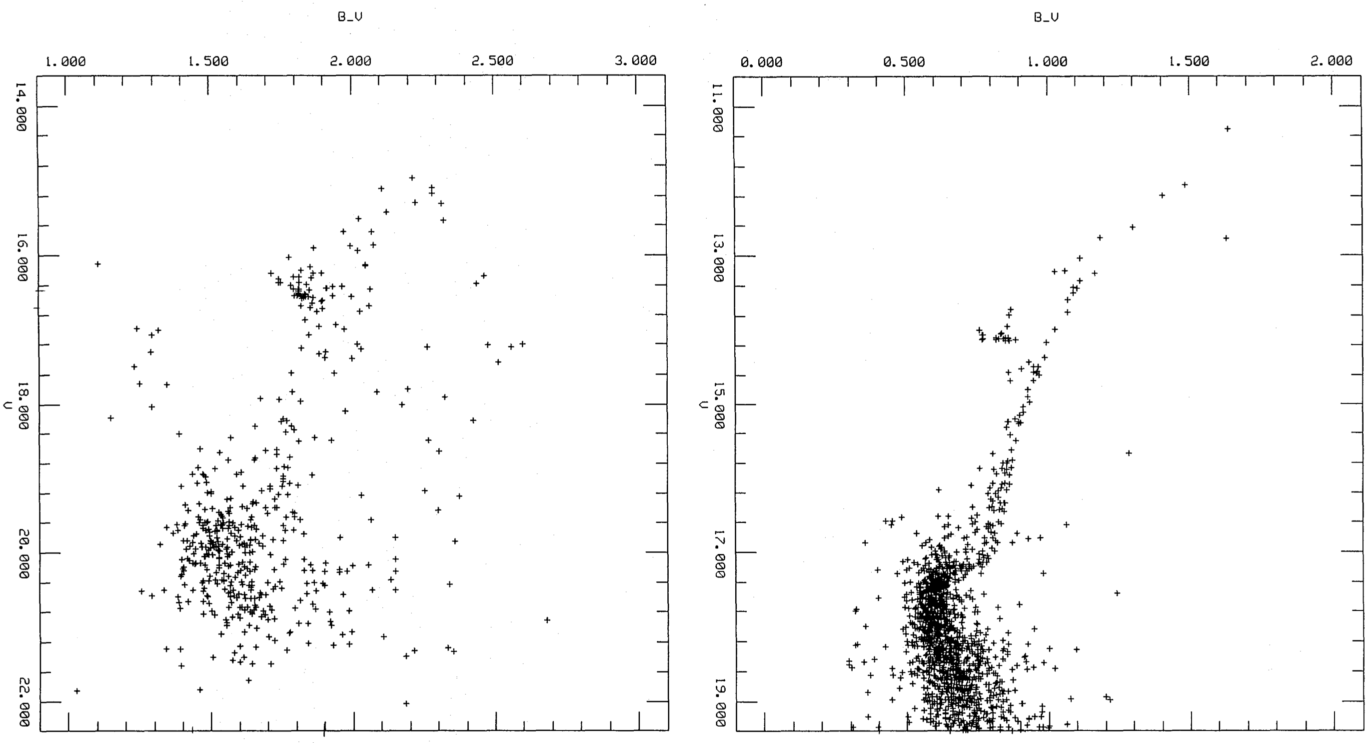

a

b

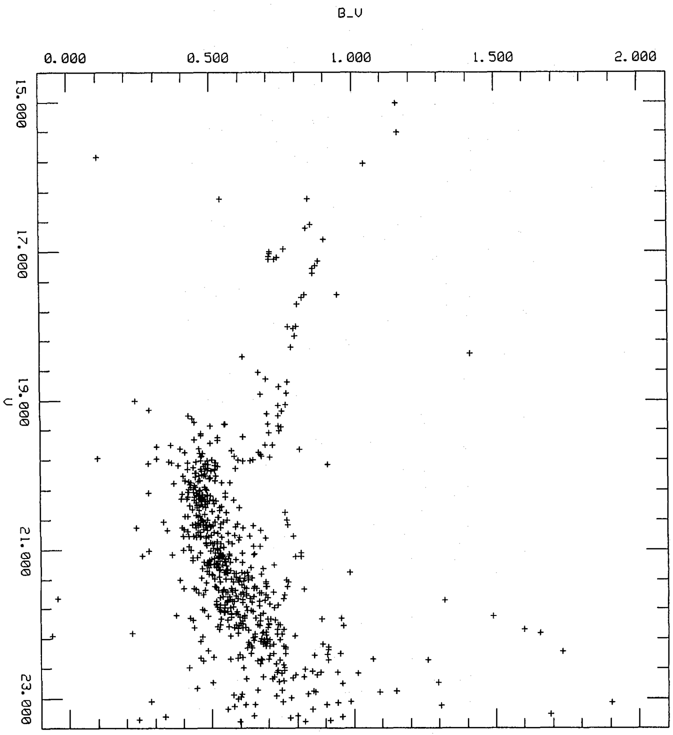

c

Fig. 9a–c. CMD in V vs. $(B-V)$ for **a** NGC 6553, where a long exposure frame, in which faint stars are measureable, was considered, and where only the lower strip of frame ($Y \lesssim 300$) was taken into account; **b** 47 Tuc (Aurière and Ortolani, 1988); **c** Pal 12 (Gratton and Ortolani, 1988)

relative to the younger intermediate age Cloud clusters as NGC 1651 in the LMC (Mould et al., 1986) and K 3 in the SMC (Rich et al., 1984).

On the other hand, it should be noted that the shape of the lower SGB seem closer to that of 47 Tuc than that of intermediate age clusters, since the younger ones show a flatter subgiant branch.

5. Concluding remarks

As pointed out by Frogel (1988), the appearance of CMDs of bulge stars cannot be inferred from the properties of the up to now well studied globular clusters of the solar neighbourhood stars. The impact of the work on NGC 6553, on the study of super-metal-rich stars, is to establish the CMD morphology for a possibly above solar metallicity cluster.

The major peculiarities observed in NGC 6553 are:

(a) Curved giant branches, where the tip of the RGB in some CMDs fall down to the magnitude level of the HB. This curvature appears to be a characteristic of SMR clusters and might be useful as a metallicity indicator. This is an important characteristic, to be considered in the study of bulges of galaxies, particularly for those within the spatial resolution of the Space Telescope.

Depending on the amount of blanketing in the spectral region, and the combination of filters, stars at the tip of the RGB can move back to the blue at fainter magnitudes [e.g., in the classical V vs. $(B-V)$ diagram], forming a hook-like structure which in extreme cases reaches the ascending RGB. In such cases, the RGB width can be misinterpreted as metallicity dispersion, photometric errors, or differential reddening. We leave here a caution for the study of CMDs of bulges of external galaxies, as well for the interpretation of observed CMDs as for the construction of population synthesis models.

(b) The anomalous tilted and very red HB is not well explained. The tilting can be produced by several effects, as differential reddening, blanketing and the possibility for the presence of the RGB clump.

Finally, the determination of the ages is very important, since it can give a clue to the kind of population to which the cluster belongs. For this purpose, better quality frames, as could be done with the Space Telescope, would be interesting. From the presently obtained data, we were able to obtain some indication on the age of NGC 6553: using the criterion of magnitude difference between HB and turn-off, the age of NGC 6553 could be slightly younger than that of classical globular clusters. On the other hand, it seems to be older than Pal 12, this latter being clearly an exceptionally young globular cluster.

Acknowledgements. We are thankful to Alvio Renzini for enthusiastic encouragement and very interesting suggestions and discussion. We are also grateful to Cesare Chiosi for discussions about theoretical isochrones for metal-rich populations, and to Giampaolo Piotto for helping with part of the observations. The ESO technical staff has been of great support in preparing the instrumentation.

B. B. acknowledges a partial support from Fapesp (São Paulo), E. B. acknowledges a fellowship from CNPq (Brazil).

References

Armandroff, T.E.: 1988, *Astron. J.* **96**, 588
Aurière, M., Ortolani, S.: 1988, *Astron. Astrophys.* **204**, 106
Bell, R.A., Gustafsson, B.: 1978, *Astron. Astrophys. Suppl.* **34**, 229
Bica, E.: 1988, *Astron. Astrophys.* **195**, 76
Bica, E., Alloin, D.: 1986a, *Astron. Astrophys.* **162**, 21
Bica, E., Alloin, D.: 1986b, *Astron. Astrophys. Suppl.* **66**, 171
Bica, E., Pastoriza, M.G.: 1983, *Astrophys. Space Sci.* **91**, 99
Buonnano, R., Corsi, C.E., Fusi-Pecci, F.: 1989, *Astron. Astrophys.* (in press)
Frogel, J.A.: 1988, *Ann. Rev. Astron. Astrophys.* **26**, 51
Frogel, J.A., Whitford, A.E.: 1987, *Astrophys. J.* **320**, 199
Fusi-Pecci, F., Ferraro, F.R., Crocker, D.A., Rood, R.T., Buonnano, R.: 1989, in *Astrophysical Ages and Dating Methods*, eds. E. Vangioni-Flam, M. Cassé, J. Audouze, Editions Frontieres (to appear)
Gratton, R.G., Tornambe, A., Ortolani, S.: 1986, *Astron. Astrophys.* **169**, 111
Gratton, R.G., Ortolani, S.: 1988, *Astron. Astrophys. Suppl.* **73**, 137
Hartwick, F.D.A.: 1975, *Publ. Astron. Soc. Pacific* **87**, 77
Hesser, J.E., Harris, W.E., Vandenberg, D.A., Allwright, J.W.B., Shott, P., Stetson, P.B.: 1987, *Publ. Astron. Soc. Pacific* **99**, 739
Hogg, H.S.: 1973, *Publ. David Dunlap Obs.* **3**, n°. 6
King, C.R., da Costa, G.S., Demarque, P.: 1985, *Astrophys. J.* **299**, 674
Landolt, A.U.: 1983, *Astron. J.* **88**, 439
Lloyd Evans, T.: 1983, *Monthly Notices Roy. Astron. Soc.* **204**, 945
Lloyd Evans, T., Menzies, J.W.: 1977, *Monthly Notices Roy. Astron. Soc.* **178**, 163
Lloyd Evans, T., Menzies, J.W.: 1973, in *Variables in Globular Clusters and Related Systems*, *IAU Coll.* **21**, ed. J.D. Fernie, Reidel, Dordrecht, p. 151
Mateo, M., Hodge, P., Schommer, T.: 1986, *Astrophys. J.* **311**, 113
Morgan, W.W.: 1959, *Astron. J.* **64**, 432
Mould, J.R., da Costa, G.S., Crawford, M.D.: 1986, *Astrophys. J.* **304**, 265
Mould, J.R.: 1986, in *Stellar Populations*, eds. C.A. Norman, A., Renzini, M. Tosi, Cambridge University Press, Cambridge, p. 9
Olszewski, E., Schommer, R., Aaronson, M.: 1987, *Astron. J.* **93**, 565
Ortolani, S.: 1989, Space Telescope Technical Report, STCF-ESO Garching
Pilachowski, C.A.: 1984, *Astrophys. J.* **281**, 614
Racine, R.: 1973, *Astron. J.* **78**, 180
Rich, M., da Costa, G.S., Mould, J.R.: 1984, *Astrophys. J.* **286**, 517
Terndrup, D.M.: 1988, *Astron. J.* **96**, 884
Van den Bergh, S.: 1967, *Astron. J.* **72**, 70
Webbink, R.F.: 1985, in *Dynamics of Star Clusters*, *IAU Symp.* **113**, eds. J. Goodman, P. Hut, Reidel, Dordrecht, p. 541
Whitford, A.E., Rich, M.: 1983, *Astrophys. J.* **274**, 723
Zinn, R.: 1980a, *Astrophys. J. Suppl.* **42**, 19
Zinn, R.: 1980b, *Astrophys. J.* **241**, 602
Zinn, R.: 1985, *Astrophys. J.* **293**, 424
Zinn, R., West, M.J.: 1984, *Astrophys. J. Suppl.* **55**, 45